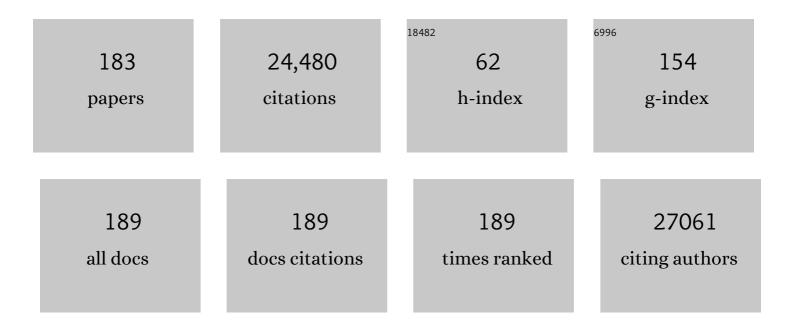
Lincoln J Lauhon

List of Publications by Year in descending order

Source: https://exaly.com/author-pdf/500647/publications.pdf Version: 2024-02-01



#	Article	IF	CITATIONS
1	GaN lateral polar junction arrays with 3D control of doping by supersaturation modulated growth: A path toward III-nitride superjunctions. Journal of Applied Physics, 2022, 131, 015703.	2.5	8
2	Allâ€Printed Ultrahighâ€Responsivity MoS ₂ Nanosheet Photodetectors Enabled by Megasonic Exfoliation. Advanced Materials, 2022, 34, .	21.0	25
3	Selective Area Regrowth Produces Nonuniform Mg Doping Profiles in Nonplanar GaN p–n Junctions. ACS Applied Electronic Materials, 2021, 3, 704-710.	4.3	8
4	Atomic-level charge transport mechanism in gate-tunable anti-ambipolar van der Waals heterojunctions. Applied Physics Letters, 2021, 118, .	3.3	8
5	Exaggerated sensitivity in photodetectors with internal gain. Nature Photonics, 2021, 15, 714-714.	31.4	12
6	(Invited) Selective Area Etching and Doping of GaN for High-Power Applications. ECS Transactions, 2021, 104, 103-112.	0.5	1
7	A New Approach to Designing High-Sensitivity Low-Dimensional Photodetectors. Nano Letters, 2021, 21, 9838-9844.	9.1	12
8	(Invited) Selective Area Etching and Doping of GaN for High-Power Applications. ECS Meeting Abstracts, 2021, MA2021-02, 996-996.	0.0	0
9	Light and complex 3D MoS ₂ /graphene heterostructures as efficient catalysts for the hydrogen evolution reaction. Nanoscale, 2020, 12, 2715-2725.	5.6	35
10	High resolution strain mapping of a single axially heterostructured nanowire using scanning X-ray diffraction. Nano Research, 2020, 13, 2460-2468.	10.4	11
11	Molecular-Scale Characterization of Photoinduced Charge Separation in Mixed-Dimensional InSe–Organic van der Waals Heterostructures. ACS Nano, 2020, 14, 3509-3518.	14.6	17
12	Emergent Optoelectronic Properties of Mixed-Dimensional Heterojunctions. Accounts of Chemical Research, 2020, 53, 763-772.	15.6	55
13	Remote Doping of Scalable Nanowire Branches. Nano Letters, 2020, 20, 3577-3584.	9.1	13
14	In Situ Transport Measurements Reveal Source of Mobility Enhancement of MoS ₂ and MoTe ₂ during Dielectric Deposition. ACS Applied Electronic Materials, 2020, 2, 1273-1279.	4.3	4
15	Strain Mapping of CdTe Grains in Photovoltaic Devices. IEEE Journal of Photovoltaics, 2019, 9, 1790-1799.	2.5	20
16	Charge Separation in Epitaxial SnS/MoS ₂ Vertical Heterojunctions Grown by Low-Temperature Pulsed MOCVD. ACS Applied Materials & Interfaces, 2019, 11, 40543-40550.	8.0	16
17	Nonlinear Mode Coupling and One-to-One Internal Resonances in a Monolayer WS ₂ Nanoresonator. Nano Letters, 2019, 19, 4052-4059.	9.1	24
18	Correlated Nanoscale Analysis of the Emission from Wurtzite versus Zincblende (In,Ga)As/GaAs Nanowire Core–Shell Quantum Wells. Nano Letters, 2019, 19, 4448-4457.	9.1	11

#	Article	IF	CITATIONS
19	Two-dimensional charge carrier distribution in MoS2 monolayer and multilayers. Applied Physics Letters, 2019, 114, .	3.3	32
20	Broad-band high-gain room temperature photodetectors using semiconductor–metal nanofloret hybrids with wide plasmonic response. Nanoscale, 2019, 11, 6368-6376.	5.6	6
21	Strain-Energy Release in Bent Semiconductor Nanowires Occurring by Polygonization or Nanocrack Formation. ACS Nano, 2019, 13, 3730-3738.	14.6	7
22	An Experimental Setup for Combined In-Vacuo Raman Spectroscopy and Cavity-Interferometry Measurements on TMDC Nano-resonators. Experimental Mechanics, 2019, 59, 349-359.	2.0	6
23	Charge confining mechanisms in III-V semiconductor nanowire. , 2019, , .		0
24	Multimodal X-ray imaging of grain-level properties and performance in a polycrystalline solar cell. Journal of Synchrotron Radiation, 2019, 26, 1316-1321.	2.4	20
25	High-Resolution Nanoscale Solid-State Nuclear Magnetic Resonance Spectroscopy. Physical Review X, 2018, 8, .	8.9	24
26	Charge Separation at Mixed-Dimensional Single and Multilayer MoS ₂ /Silicon Nanowire Heterojunctions. ACS Applied Materials & Interfaces, 2018, 10, 16760-16767.	8.0	31
27	Self-Aligned van der Waals Heterojunction Diodes and Transistors. Nano Letters, 2018, 18, 1421-1427.	9.1	51
28	Correlated Chemical and Electrically Active Dopant Analysis in Catalyst-Free Si-Doped InAs Nanowires. ACS Nano, 2018, 12, 1603-1610.	14.6	13
29	Measuring Three-Dimensional Strain and Structural Defects in a Single InGaAs Nanowire Using Coherent X-ray Multiangle Bragg Projection Ptychography. Nano Letters, 2018, 18, 811-819.	9.1	80
30	Template-Assisted Scalable Nanowire Networks. Nano Letters, 2018, 18, 2666-2671.	9.1	92
31	Criteria and considerations for preparing atom-probe tomography specimens of nanomaterials utilizing an encapsulation methodology. Ultramicroscopy, 2018, 184, 225-233.	1.9	13
32	Doping of Self-Catalyzed Nanowires under the Influence of Droplets. Nano Letters, 2018, 18, 81-87.	9.1	24
33	Suppressing Ambient Degradation of Exfoliated InSe Nanosheet Devices via Seeded Atomic Layer Deposition Encapsulation. Nano Letters, 2018, 18, 7876-7882.	9.1	54
34	Perspectives on frontiers in electronic and photonic materials. MRS Bulletin, 2018, 43, 901-908.	3.5	0
35	Tuning Lasing Emission toward Long Wavelengths in GaAs-(In,Al)GaAs Core–Multishell Nanowires. Nano Letters, 2018, 18, 6292-6300.	9.1	43
36	Atom probe tomography of nanoscale architectures in functional materials for electronic and photonic applications. Current Opinion in Solid State and Materials Science, 2018, 22, 171-187.	11.5	5

#	Article	IF	CITATIONS
37	Atomic Layer Deposition of Molybdenum Oxides with Tunable Stoichiometry Enables Controllable Doping of MoS ₂ . Chemistry of Materials, 2018, 30, 3628-3632.	6.7	29
38	He-Ion Microscopy as a High-Resolution Probe for Complex Quantum Heterostructures in Core–Shell Nanowires. Nano Letters, 2018, 18, 3911-3919.	9.1	13
39	Connecting Composition-Driven Faceting with Facet-Driven Composition Modulation in GaAs–AlGaAs Core–Shell Nanowires. Nano Letters, 2018, 18, 5179-5185.	9.1	13
40	(Invited) Variable Doping of MoS2 By Atomic Layer Deposition of Molybdenum Oxides of Controlled Stochiometry. ECS Meeting Abstracts, 2018, , .	0.0	0
41	Evolutionary Design and Prototyping of Single Crystalline Titanium Nitride Lattice Optics. ACS Photonics, 2017, 4, 606-612.	6.6	40
42	Lowâ€Temperature Atomic Layer Deposition of MoS ₂ Films. Angewandte Chemie, 2017, 129, 5073-5077.	2.0	15
43	Identifying Excitation and Emission Rate Contributions to Plasmon-Enhanced Photoluminescence from Monolayer MoS ₂ Using a Tapered Gold Nanoantenna. ACS Photonics, 2017, 4, 1602-1606.	6.6	17
44	Lowâ€Temperature Atomic Layer Deposition of MoS ₂ Films. Angewandte Chemie - International Edition, 2017, 56, 4991-4995.	13.8	127
45	Enhanced radiative emission from monolayer MoS2 films using a single plasmonic dimer nanoantenna. Applied Physics Letters, 2017, 111, .	3.3	23
46	Quantum Transport and Sub-Band Structure of Modulation-Doped GaAs/AlAs Core–Superlattice Nanowires. Nano Letters, 2017, 17, 4886-4893.	9.1	18
47	Truly Electroformingâ€Free and Lowâ€Energy Memristors with Preconditioned Conductive Tunneling Paths. Advanced Functional Materials, 2017, 27, 1702010.	14.9	75
48	1-D Metal Nanobead Arrays within Encapsulated Nanowires via a Red-Ox-Induced Dewetting: Mechanism Study by Atom-Probe Tomography. Nano Letters, 2017, 17, 7478-7486.	9.1	4
49	Nanowire Kinking Modulates Doping Profiles by Reshaping the Liquid–Solid Growth Interface. Nano Letters, 2017, 17, 4518-4525.	9.1	16
50	Control of interlayer physics in 2H transition metal dichalcogenides. Journal of Applied Physics, 2017, 122, .	2.5	21
51	Epitaxial Heterostructure Nanowires. , 2017, , 3-29.		Ο
52	Suppression of alloy fluctuations in GaAs-AlGaAs core-shell nanowires. Applied Physics Letters, 2016, 109, .	3.3	17
53	Dopant Diffusion and Activation in Silicon Nanowires Fabricated by ex Situ Doping: A Correlative Study via Atom-Probe Tomography and Scanning Tunneling Spectroscopy. Nano Letters, 2016, 16, 4490-4500.	9.1	36
54	Atom Probe Tomography Analysis of Ag Doping in 2D Layered Material (PbSe) ₅ (Bi ₂ Se ₃) ₃ . Nano Letters, 2016, 16, 6064-6069.	9.1	8

#	Article	IF	CITATIONS
55	Metal-Free Carbon-Based Nanomaterial Coatings Protect Silicon Photoanodes in Solar Water-Splitting. Nano Letters, 2016, 16, 7370-7375.	9.1	30
56	Plasmonic Lattice Lenses for Multiwavelength Achromatic Focusing. ACS Nano, 2016, 10, 10275-10282.	14.6	80
57	Hybrid, Gate-Tunable, van der Waals p–n Heterojunctions from Pentacene and MoS ₂ . Nano Letters, 2016, 16, 497-503.	9.1	295
58	Impact of Dopant Compensation on Graded <i>p</i> – <i>n</i> Junctions in Si Nanowires. ACS Applied Materials & Interfaces, 2016, 8, 128-134.	8.0	8
59	Atom Probe Tomography of Nanowires. Semiconductors and Semimetals, 2015, , 249-278.	0.7	4
60	Large-Area, Low-Voltage, Antiambipolar Heterojunctions from Solution-Processed Semiconductors. Nano Letters, 2015, 15, 416-421.	9.1	87
61	Spin transport and Hanle effect in silicon nanowires using graphene tunnel barriers. Nature Communications, 2015, 6, 7541.	12.8	26
62	Alloy Fluctuations Act as Quantum Dot-like Emitters in GaAs-AlGaAs Core–Shell Nanowires. ACS Nano, 2015, 9, 8335-8343.	14.6	65
63	Demonstration of Confined Electron Gas and Steep-Slope Behavior in Delta-Doped GaAs-AlGaAs Core–Shell Nanowire Transistors. Nano Letters, 2015, 15, 3295-3302.	9.1	60
64	Investigation of Band-Offsets at Monolayer–Multilayer MoS ₂ Junctions by Scanning Photocurrent Microscopy. Nano Letters, 2015, 15, 2278-2284.	9.1	141
65	Gate-tunable memristive phenomena mediated by grain boundaries in single-layer MoS2. Nature Nanotechnology, 2015, 10, 403-406.	31.5	564
66	Correlated high-resolution x-ray diffraction, photoluminescence, and atom probe tomography analysis of continuous and discontinuous InxGa1â^'xN quantum wells. Applied Physics Letters, 2015, 107,	3.3	10
67	Optical Control of Mechanical Mode-Coupling within a MoS ₂ Resonator in the Strong-Coupling Regime. Nano Letters, 2015, 15, 6727-6731.	9.1	55
68	Rational Control of Diffraction and Interference from Conformal Phase Gratings: Toward Highâ€Resolution 3D Nanopatterning. Advanced Optical Materials, 2014, 2, 1213-1220.	7.3	33
69	Wafer-scale solution-derived molecular gate dielectrics for low-voltage graphene electronics. Applied Physics Letters, 2014, 104, .	3.3	22
70	On the reliable analysis of indium mole fraction within InxGa1â^'xN quantum wells using atom probe tomography. Applied Physics Letters, 2014, 104, 152102.	3.3	35
71	Extraordinary Dynamic Mechanical Response of Vanadium Dioxide Nanowires around the Insulator to Metal Phase Transition. Nano Letters, 2014, 14, 1898-1902.	9.1	45
72	Emerging Device Applications for Semiconducting Two-Dimensional Transition Metal Dichalcogenides. ACS Nano, 2014, 8, 1102-1120.	14.6	2,307

#	Article	IF	CITATIONS
73	Subwavelength Lattice Optics by Evolutionary Design. Nano Letters, 2014, 14, 7195-7200.	9.1	73
74	Effective Passivation of Exfoliated Black Phosphorus Transistors against Ambient Degradation. Nano Letters, 2014, 14, 6964-6970.	9.1	1,294
75	Lift-out procedures for atom probe tomography targeting nanoscale features in core-shell nanowire heterostructures. Physica Status Solidi C: Current Topics in Solid State Physics, 2014, 11, 656-661.	0.8	17
76	Influence of Stoichiometry on the Optical and Electrical Properties of Chemical Vapor Deposition Derived MoS ₂ . ACS Nano, 2014, 8, 10551-10558.	14.6	281
77	In Situ Electron Microscopy Fourâ€Point Electromechanical Characterization of Freestanding Metallic and Semiconducting Nanowires. Small, 2014, 10, 725-733.	10.0	40
78	Energy Frontier Research Center for Solid-State Lighting Science: Exploring New Materials Architectures and Light Emission Phenomena. Journal of Physical Chemistry C, 2014, 118, 13330-13345.	3.1	12
79	Elucidating the Photoresponse of Ultrathin MoS ₂ Field-Effect Transistors by Scanning Photocurrent Microscopy. Journal of Physical Chemistry Letters, 2013, 4, 2508-2513.	4.6	190
80	Origin of Polytype Formation in VLS-Grown Ge Nanowires through Defect Generation and Nanowire Kinking. Nano Letters, 2013, 13, 3947-3952.	9.1	40
81	Spatial Mapping of Efficiency of GaN/InGaN Nanowire Array Solar Cells Using Scanning Photocurrent Microscopy. Nano Letters, 2013, 13, 5123-5128.	9.1	76
82	Barrier Height Measurement of Metal Contacts to Si Nanowires Using Internal Photoemission of Hot Carriers. Nano Letters, 2013, 13, 6183-6188.	9.1	31
83	Demonstration of an Electrochemical Liquid Cell for Operando Transmission Electron Microscopy Observation of the Lithiation/Delithiation Behavior of Si Nanowire Battery Anodes. Nano Letters, 2013, 13, 6106-6112.	9.1	265
84	Three-Dimensional Mapping of Quantum Wells in a GaN/InGaN Core–Shell Nanowire Light-Emitting Diode Array. Nano Letters, 2013, 13, 4317-4325.	9.1	96
85	Band-like transport in high mobility unencapsulated single-layer MoS2 transistors. Applied Physics Letters, 2013, 102, .	3.3	359
86	Electron-Rich Driven Electrochemical Solid-State Amorphization in Li–Si Alloys. Nano Letters, 2013, 13, 4511-4516.	9.1	51
87	ldentification of an Intrinsic Source of Doping Inhomogeneity in Vapor–Liquid–Solid-Grown Nanowires. Nano Letters, 2013, 13, 199-206.	9.1	54
88	Carbon nanomaterials for electronics, optoelectronics, photovoltaics, and sensing. Chemical Society Reviews, 2013, 42, 2824-2860.	38.1	1,105
89	Electron Tomography of Au-Catalyzed Semiconductor Nanowires. Journal of Physical Chemistry C, 2013, 117, 1059-1063.	3.1	12
90	Spatially Resolved Correlation of Active and Total Doping Concentrations in VLS Grown Nanowires. Nano Letters, 2013, 13, 2598-2604.	9.1	40

#	Article	IF	CITATIONS
91	Quantitatively Enhanced Reliability and Uniformity of High-κ Dielectrics on Graphene Enabled by Self-Assembled Seeding Layers. Nano Letters, 2013, 13, 1162-1167.	9.1	67
92	Nanowire Heterostructures. Annual Review of Materials Research, 2013, 43, 451-479.	9.3	140
93	High-Field Transport and Thermal Reliability of Sorted Carbon Nanotube Network Devices. ACS Nano, 2013, 7, 482-490.	14.6	35
94	Electronic Origin for the Phase Transition from Amorphous Li _{<i>x</i>} Si to Crystalline Li ₁₅ Si ₄ . ACS Nano, 2013, 7, 6303-6309.	14.6	135
95	Low-Frequency Electronic Noise in Single-Layer MoS ₂ Transistors. Nano Letters, 2013, 13, 4351-4355.	9.1	221
96	Largeâ€Area, Electronically Monodisperse, Aligned Singleâ€Walled Carbon Nanotube Thin Films Fabricated by Evaporationâ€Driven Selfâ€Assembly. Small, 2013, 9, 45-51.	10.0	67
97	Near-field microwave microscopy of high- <i>κ</i> oxides grown on graphene with an organic seeding layer. Applied Physics Letters, 2013, 103, .	3.3	12
98	Publisher's Note: Nanoscale Fourier-Transform Magnetic Resonance Imaging [Phys. Rev. X 3 , 031016 (2013)]. Physical Review X, 2013, 3, .	8.9	3
99	Nanoscale Fourier-Transform Magnetic Resonance Imaging. Physical Review X, 2013, 3, .	8.9	27
100	Extrinsic and intrinsic photoresponse in monodisperse carbon nanotube thin film transistors. Applied Physics Letters, 2013, 102, .	3.3	8
101	Gate-tunable carbon nanotube–MoS ₂ heterojunction p-n diode. Proceedings of the National Academy of Sciences of the United States of America, 2013, 110, 18076-18080.	7.1	373
102	Raman concentrators in Ge nanowires with dielectric coatings. Optics Express, 2012, 20, 5127.	3.4	4
103	Nanomechanical detection of nuclear magnetic resonance using a silicon nanowire oscillator. Physical Review B, 2012, 85, .	3.2	76
104	A Method for Directly Correlating Site-Specific Cross-Sectional and Plan-View Transmission Electron Microscopy of Individual Nanostructures. Microscopy and Microanalysis, 2012, 18, 1410-1418.	0.4	10
105	Increased Yield and Uniformity of Vanadium Dioxide Nanobeam Growth via Two-Step Physical Vapor Transport Process. Crystal Growth and Design, 2012, 12, 1383-1387.	3.0	27
106	Correlation and Morphology of Dopant Decomposition in Mn and Co Codoped Ge Epitaxial Films. Journal of Physical Chemistry C, 2012, 116, 276-280.	3.1	7
107	Direct Measurements of Lateral Variations of Schottky Barrier Height Across "End-On―Metal Contacts to Vertical Si Nanowires by Ballistic Electron Emission Microscopy. Nano Letters, 2012, 12, 694-698.	9.1	6
108	Quantitative Statistical Analysis of Dielectric Breakdown in Zirconia-Based Self-Assembled Nanodielectrics. ACS Nano, 2012, 6, 4452-4460.	14.6	9

#	Article	IF	CITATIONS
109	Atom Probe Tomography of <i>a</i> -Axis GaN Nanowires: Analysis of Nonstoichiometric Evaporation Behavior. ACS Nano, 2012, 6, 3898-3906.	14.6	72
110	Catalyst Incorporation at Defects during Nanowire Growth. Nano Letters, 2012, 12, 167-171.	9.1	58
111	Fundamental Performance Limits of Carbon Nanotube Thin-Film Transistors Achieved Using Hybrid Molecular Dielectrics. ACS Nano, 2012, 6, 7480-7488.	14.6	142
112	Atomic Structural Analysis of Nanowire Defects and Polytypes Enabled Through Cross‧ectional Lattice Imaging. Small, 2012, 8, 1717-1724.	10.0	13
113	Diameter and Polarization-Dependent Raman Scattering Intensities of Semiconductor Nanowires. Nano Letters, 2012, 12, 2266-2271.	9.1	42
114	Stoichiometry Engineering of Monoclinic to Rutile Phase Transition in Suspended Single Crystalline Vanadium Dioxide Nanobeams. Nano Letters, 2011, 11, 1443-1447.	9.1	157
115	Atypical Self-Activation of Ga Dopant for Ge Nanowire Devices. Nano Letters, 2011, 11, 3108-3112.	9.1	16
116	Obtaining Uniform Dopant Distributions in VLS-Grown Si Nanowires. Nano Letters, 2011, 11, 183-187.	9.1	81
117	Silicon Nanowire Polytypes: Identification by Raman Spectroscopy, Generation Mechanism, and Misfit Strain in Homostructures. ACS Nano, 2011, 5, 8958-8966.	14.6	66
118	Spatially Resolved Plasmonically Enhanced Photocurrent from Au Nanoparticles on a Si Nanowire. Nano Letters, 2011, 11, 2731-2734.	9.1	63
119	Direct Measurement of Individual Deep Traps in Single Silicon Nanowires. Nano Letters, 2011, 11, 2499-2502.	9.1	39
120	Direct measurement of nanowire Schottky junction depletion region. Applied Physics Letters, 2011, 99, 223511.	3.3	23
121	Direct Measurement of Inhomogeneous Longitudinal Dopant Distribution in SiNWs Using Nano-Probe Scanning Auger Microscopy Materials Research Society Symposia Proceedings, 2011, 1349, 142101.	0.1	0
122	Texture analysis of manganese-germanide/germanium nanowire heterostructures by high resolution electron microscopy and diffraction. Journal of Materials Research, 2011, 26, 2299-2304.	2.6	3
123	Mitigation of surface doping in VLS-grown Si nanowires. , 2010, , .		1
124	Broadband Plasmonic Microlenses Based on Patches of Nanoholes. Nano Letters, 2010, 10, 4111-4116.	9.1	120
125	Direct Detection of Hole Gas in Geâ^'Si Coreâ^'Shell Nanowires by Enhanced Raman Scattering. Nano Letters, 2010, 10, 4483-4487.	9.1	34
126	Weibull Analysis of Dielectric Breakdown in a Self-Assembled Nanodielectric for Organic Transistors. Journal of Physical Chemistry Letters, 2010, 1, 3292-3297.	4.6	38

#	Article	IF	CITATIONS
127	Growth of Ge Nanowires from Auâ^'Cu Alloy Nanoparticle Catalysts Synthesized from Aqueous Solution. Journal of Physical Chemistry Letters, 2010, 1, 3360-3365.	4.6	23
128	Tomographic study of atomic-scale redistribution of platinum during the silicidation of Ni0.95Pt0.05/Si(100) thin films. Applied Physics Letters, 2009, 94, 113103.	3.3	17
129	Nonuniform doping distribution along silicon nanowires measured by Kelvin probe force microscopy and scanning photocurrent microscopy. Applied Physics Letters, 2009, 95, .	3.3	84
130	Controlling the nonlinearity of silicon nanowire resonators using active feedback. Applied Physics Letters, 2009, 95, 123116.	3.3	32
131	Correlating dopant distributions and electrical properties of boron-doped silicon nanowires. Applied Physics Letters, 2009, 95, .	3.3	44
132	Atom-Probe Tomography of Semiconductor Materials and Device Structures. MRS Bulletin, 2009, 34, 738-743.	3.5	42
133	Nonuniform Nanowire Doping Profiles Revealed by Quantitative Scanning Photocurrent Microscopy. Advanced Materials, 2009, 21, 3067-3072.	21.0	113
134	A synergistic assembly of nanoscale lamellar photoconductor hybrids. Nature Materials, 2009, 8, 68-75.	27.5	174
135	Direct measurement of dopant distribution in an individual vapour–liquid–solid nanowire. Nature Nanotechnology, 2009, 4, 315-319.	31.5	379
136	Relative Influence of Surface States and Bulk Impurities on the Electrical Properties of Ge Nanowires. Nano Letters, 2009, 9, 3268-3274.	9.1	115
137	Direct Correlation of Structural Domain Formation with the Metal Insulator Transition in a VO ₂ Nanobeam. Nano Letters, 2009, 9, 4527-4532.	9.1	195
138	Vanadium oxide nanowire phase and orientation analyzed by Raman spectroscopy. Journal of Applied Physics, 2009, 105, .	2.5	64
139	Alternative catalysts for VSS growth of silicon and germanium nanowires. Journal of Materials Chemistry, 2009, 19, 849.	6.7	136
140	Ordered Stacking Fault Arrays in Silicon Nanowires. Nano Letters, 2009, 9, 2774-2779.	9.1	113
141	Scanning Photocurrent Microscopy Analysis of Si Nanowire Field-Effect Transistors Fabricated by Surface Etching of the Channel. Nano Letters, 2009, 9, 1903-1908.	9.1	44
142	Three-Dimensional Atom-Probe Tomographic Studies of Nickel Monosilicide/Silicon Interfaces on a Subnanometer Scale. ECS Transactions, 2009, 19, 303-314.	0.5	7
143	Tomographic analysis of dilute impurities in semiconductor nanostructures. Journal of Solid State Chemistry, 2008, 181, 1642-1649.	2.9	62
144	High-resolution detection of Au catalyst atoms in Si nanowires. Nature Nanotechnology, 2008, 3, 168-173.	31.5	575

#	Article	IF	CITATIONS
145	Syntaxial Growth of Ge/Mn-Germanide Nanowire Heterostructures. Nano Letters, 2008, 8, 2669-2673.	9.1	32
146	Displacement detection of silicon nanowires by polarization-enhanced fiber-optic interferometry. Applied Physics Letters, 2008, 93, .	3.3	76
147	Three-dimensional atomic-scale mapping of Pd in Ni1â^'xPdxSiâ^•Si(100) thin films. Applied Physics Letters, 2007, 91, 113106.	3.3	17
148	Quantitative characterization of carrier transport in nanowire photodetectors. , 2007, , .		0
149	Vaporâ^'Solidâ^'Solid Synthesis of Ge Nanowires from Vapor-Phase-Deposited Manganese Germanide Seeds. Journal of the American Chemical Society, 2007, 129, 10670-10671.	13.7	44
150	Space-charge-limited current in nanowires depleted by oxygen adsorption. Applied Physics Letters, 2006, 89, 143102.	3.3	90
151	Three-Dimensional Nanoscale Composition Mapping of Semiconductor Nanowires. Nano Letters, 2006, 6, 181-185.	9.1	214
152	Low-temperature photoluminescence imaging and time-resolved spectroscopy of single CdS nanowires. Applied Physics Letters, 2006, 89, 053119.	3.3	38
153	Quantitative Measurement of the Electron and Hole Mobilityâ^'Lifetime Products in Semiconductor Nanowires. Nano Letters, 2006, 6, 948-952.	9.1	95
154	Resonant Raman scattering from CdS nanowires. Applied Physics Letters, 2006, 88, 043118.	3.3	39
155	Ferromagnetic Self-Assembled Quantum Dots on Semiconductor Nanowires. Nano Letters, 2006, 6, 50-54.	9.1	59
156	Composition analysis of single semiconductor nanowires using pulsed-laser atom probe tomography. Applied Physics A: Materials Science and Processing, 2006, 85, 271-275.	2.3	47
157	Temperature dependent photoluminescence of single CdS nanowires. Applied Physics Letters, 2006, 89, 123123.	3.3	56
158	Local photocurrent mapping as a probe of contact effects and charge carrier transport in semiconductor nanowire devices. Journal of Vacuum Science & Technology B, 2006, 24, 2172.	1.3	36
159	Dendritic Nanowire Growth Mediated by a Self-Assembled Catalyst. Advanced Materials, 2005, 17, 598-602.	21.0	94
160	Near-field scanning photocurrent microscopy of a nanowire photodetector. Applied Physics Letters, 2005, 87, 043111.	3.3	196
161	Growth and transport properties of complementary germanium nanowire field-effect transistors. Applied Physics Letters, 2004, 84, 4176-4178.	3.3	351
162	Semiconductor nanowire heterostructures. Philosophical Transactions Series A, Mathematical, Physical, and Engineering Sciences, 2004, 362, 1247-1260.	3.4	220

#	Article	IF	CITATIONS
163	STM Images and Chemisorption Bond Parameters of Acetylene, Ethynyl, and Dicarbon Chemisorbed on Copperâ€. Journal of Physical Chemistry B, 2002, 106, 8161-8171.	2.6	32
164	Epitaxial core–shell and core–multishell nanowire heterostructures. Nature, 2002, 420, 57-61.	27.8	1,980
165	Growth of nanowire superlattice structures for nanoscale photonics and electronics. Nature, 2002, 415, 617-620.	27.8	2,562
166	Diameter-controlled synthesis of single-crystal silicon nanowires. Applied Physics Letters, 2001, 78, 2214-2216.	3.3	1,078
167	Effects of temperature and other experimental variables on single molecule vibrational spectroscopy with the scanning tunneling microscope. Review of Scientific Instruments, 2001, 72, 216-223.	1.3	113
168	Inducing and Observing the Abstraction of a Single Hydrogen Atom in Bimolecular Reactions with a Scanning Tunneling Microscope. Journal of Physical Chemistry B, 2001, 105, 3987-3992.	2.6	32
169	Direct comparisons of rates for low temperature diffusion of hydrogen and deuterium on Cu(001) from quantum mechanical calculations and scanning tunneling microscopy experiments. Journal of Chemical Physics, 2001, 115, 5620-5624.	3.0	47
170	Logic Gates and Computation from Assembled Nanowire Building Blocks. Science, 2001, 294, 1313-1317.	12.6	2,056
171	Symmetry Selection Rules for Vibrationally Inelastic Tunneling. Physical Review Letters, 2001, 86, 2593-2596.	7.8	182
172	Direct Observation of the Quantum Tunneling of Single Hydrogen Atoms with a Scanning Tunneling Microscope. Physical Review Letters, 2000, 85, 4566-4569.	7.8	241
173	Electronic and vibrational excitation of single molecules with a scanning tunneling microscope. Surface Science, 2000, 451, 219-225.	1.9	64
174	Vibrationally Mediated Negative Differential Resistance in a Single Molecule. Physical Review Letters, 2000, 85, 1918-1921.	7.8	194
175	Control and Characterization of a Multistep Unimolecular Reaction. Physical Review Letters, 2000, 84, 1527-1530.	7.8	104
176	The initiation and characterization of single bimolecular reactions with a scanning tunneling microscope. Faraday Discussions, 2000, 117, 249-255.	3.2	23
177	Single-Molecule Chemistry and Vibrational Spectroscopy:  Pyridine and Benzene on Cu(001). Journal of Physical Chemistry A, 2000, 104, 2463-2467.	2.5	162
178	Single-molecule vibrational spectroscopy and microscopy:â€,CO on Cu(001) and Cu(110). Physical Review B, 1999, 60, R8525-R8528.	3.2	157
179	Single molecule thermal rotation and diffusion: Acetylene on Cu(001). Journal of Chemical Physics, 1999, 111, 5633-5636.	3.0	67
180	Large Area Supersonic Jet Epitaxy of AlN, GaN, and SiC on Silicon. Materials Research Society Symposia Proceedings, 1996, 449, 277.	0.1	1

#	Article	lF	CITATIONS
181	Supersonic jet epitaxy of aluminum nitride on silicon (100). Journal of Applied Physics, 1996, 79, 7667-7671.	2.5	23
182	Langevin-like giant magnetoresistance in Co-Cu superlattices. Physical Review B, 1994, 49, 1521-1523.	3.2	62
183	High-Field Giant Magnetoresistance in Co-Cu Superlattices. Materials Research Society Symposia Proceedings, 1993, 313, 35.	0.1	4